FULL PAPER doi.org/10.1002/adsc.202100260

Advanced Synthesis & Catalysis

Chemodivergent Photocatalytic Synthesis of Dihydrofurans and β,γ-Unsaturated Ketones

Arianna Quintavalla,[a,*] Ruben Veronesi,[a] Davide Carboni,[a] Ada Martinelli,[a] Nelsi Zaccheroni,[a] Liviana Mummolo,[a] and Marco Lombardo[a,*]

[a] Alma Mater Studiorum – University of Bologna, Department of Chemistry "G. Ciamician", Via Selmi 2, 40126 Bologna, Italy
E-mail: arianna.quintavalla@unibo.it; marco.lombardo@unibo.it

Manuscript received: February 27, 2021; Revised manuscript received: April 9, 2021;
Version of record online: May 4, 2021

Supporting information for this article is available on the WWW under https://doi.org/10.1002/adsc.202100260

Abstract: A synthetic procedure, catalysed by $Ir(ppy)_3$ under visible-light irradiation, for the chemodivergent synthesis of 2,3-dihydrofurans (**3**) or β,γ-unsaturated ketones (**7**) starting from α-halo ketones (**1**) and alkenes (**2**) has been developed. The mild reaction conditions and the redox-neutral nature of the process make it particularly sustainable avoiding the use of both sacrificial reactants and stoichiometric strong oxidants. Careful experimental investigations, supported by DFT calculations, allowed to disclose in details a possible mechanistic pathway and to direct the synthesis chemodivergently either toward **3** or **7**, depending not only on the nature of the substrates, but also on the choice of the experimental conditions.

Keywords: photocatalysis; dihydrofurans; β,γ-unsaturated ketones; chemodivergent; DFT; iridium; heterocycles

Introduction

Dihydrofurans are important five-membered heterocyclic scaffolds which widely appear in natural products,[1] drugs and medicinally relevant compounds,[2] materials and dyes[3] (Figure 1). In addition, they are usefully exploited as synthetic intermediates[4] or reactants for the preparation of materials.[5] For these reasons, the synthesis of both 2,3- and 2,5-dihydrofurans has attracted much interest in the past decades and still today, as demonstrated by the high number of protocols proposed in the last two years. Several different synthetic strategies have been developed.[4a,6] In particular, the most employed approach to the construction of substituted 2,3-dihydrofurans is the [3+2] annulation, accomplished through many different protocols. Among the traditional methods we can mention the "interrupted" Feist-Bénary reaction,[7] the oxidative coupling reaction between 1,3-dicarbonyl compounds and olefins mediated by stoichiometric manganese(III),[8] cerium (IV),[8d,9a–b] or copper(II),[9c] the 1,3-dipolar reaction involving diazocarbonyl compounds and alkenes cata-

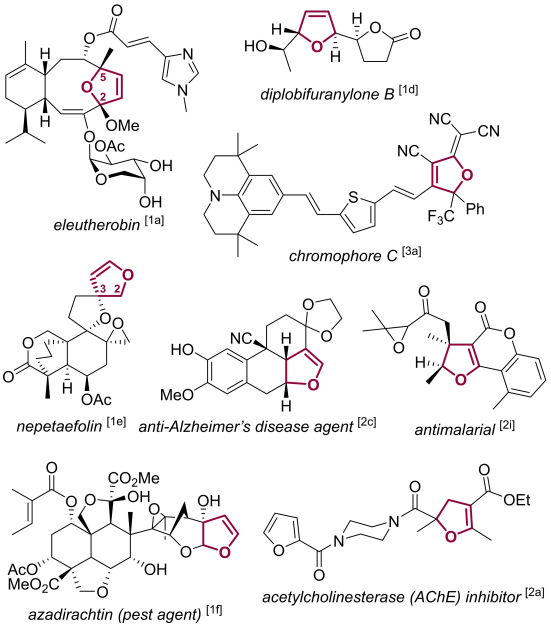

Figure 1. Notable 2,3- and 2,5-dihydrofurans.

lyzed by rhodium(II),[10] ruthenium(II),[11] or copper (II).[12] More recently, some innovative examples of [3 + 2] annulations have been proposed: i) the reaction between ketones and alkenes mediated by copper,[13] palladium,[14] or potassium persulfate,[15] by cooperative systems indium(III)/silver(I)[16] or I_2/oxidant,[17] or electrochemically promoted;[18] ii) several base-promoted additions to functionalized olefins,[19] alkynyl systems,[20] or carbonyls;[21] iii) Morita–Baylis–Hillman-type annulations;[22] iv) some copper-catalyzed formal cycloadditions involving active methylene compounds and unusual acceptors;[23] v) gold(I)-catalyzed syntheses of silyl-2,3-dihydrofurans.[24]

Some approaches different from [3 + 2] annulation have also been described for 2,3-dihydrofurans construction, as for example the cyclization of olefinic dicarbonyl compounds,[25] catalytic [4 + 1] cycloadditions,[26] the ring opening of cyclopropanes[27] or cyclopropenes,[28] the arylation of 2,5-dihydrofurans.[29] Although remarkable results have been obtained, each of the reported protocols has its own merits and demerits. In particular, almost all the published methods require stoichiometric amounts of transition metals or high catalyst loadings (with related cost and toxicity concerns), a large excess of a substrate, suitable substituted reagents, harsh reaction conditions (high temperature and/or strongly acidic solvent), and, in many cases, stoichiometric or excess of an additional strong oxidant. These disadvantages result in a poor functional group compatibility, which hinders a wide application of these protocols. Therefore, there is still a need for sustainable and flexible transformations that exceed these limitations.

As part of our ten years research interests in the synthesis of bioactive heterocyclic molecules,[30] we envisioned that a redox-neutral photocatalytic approach could be usefully applied to the synthesis of substituted 2,3-dihydrofurans. The photochemistry applied to organic synthesis has undergone a big boost over the past 10 years.[31] The use of visible light as green energy source, through an energetically controlled irradiation, has enabled mild and selective activation of photocatalysts or substrate-catalyst complexes. Indeed, compared to ultraviolet irradiation, the transparent properties of most organic substrates for visible light minimize the side reactions. It has resulted in the development of several photocatalyzed economical and environmentally benign transformations occurring under mild conditions, without the need of a special instrument or apparatus, and with great tolerance of functional groups. Moreover, visible light photochemistry has demonstrated to give access to peculiar reactivities and, in particular, to environmentally friendly free radical reactions, avoiding the traditionally employed toxic and hazardous initiators or reagents. We decided to exploit the advantages of visible light photocatalysis to develop an efficient radical synthetic approach to substituted 2,3-dihydrofurans (Scheme 1c), occurring under mild reaction conditions with low photocatalyst loading, starting from olefins and α-haloketones as easily accessible and stable substrates, avoiding large excesses of reagents and, most important, in the absence of additives or additional strong oxidants (redox-neutral conditions). Scheffer proposed in 2005 the photorearrangement of *syn*-7-benzoylnorbornene derivatives leading to *cis*-fused 2,3-dihydrofurans.[32] However, this photochemical transformation was intramolecular and promoted by high-energy UV-irradiation, showing a limited substrate scope. Afterwards, some photocatalyzed intermolecular reactions between olefins and α-halo (or α-acetoxy) carbonyls were proposed to synthesize lactones,[33] γ-hydroxyketones[34] or furans[35] (Scheme 1a). In particular, Wu[35b] and Zhu[35c] failed to avoid aromatization to furans and, therefore, they were unable to provide 2,3-dihydrofurans. The aromatization leading to furans is a major drawback of many synthetic approaches to dihydrofurans.[13a,36] Only Greaney *et al.* proposed a photoredox catalytic reaction between bromoesters or bromonitriles and styrenes obtaining the corresponding γ-hydroxy derivatives.[37] Among the tested substrates, a single α-bromo-β-ketoester was employed providing some 2,3-dihydrofurans (Scheme 1b). However, these products were sometimes accompanied by a comparable amount of the corresponding lactones. In addition, to reach acceptable yields the protocol required the use of a

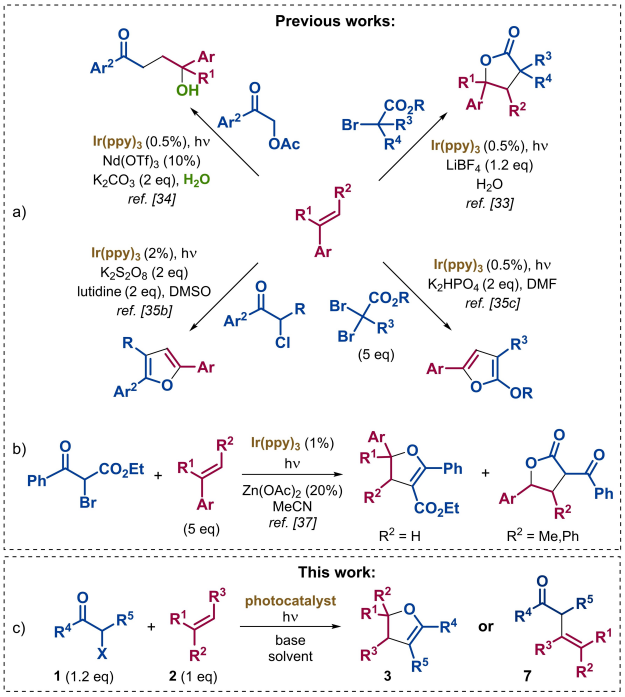

Scheme 1. Photoredox catalytic reactions between olefins and α-halo or α-acetoxy carbonyls.

large excess of olefin (5 equivalents) and of $Zn(OAc)_2$ as additive in 20 mol% amount.

Results and Discussion

Protocol optimization. Our preliminary investigations focused on the reaction between methyl 2-bromo-3-oxobutanoate **1a** and 1,1-diphenylethylene **2a** promoted by $Ru(bpy)_3Cl_2$ as photocatalyst (Table 1, entries 1–6). We were delighted by the formation of the desired 2,3-dihydrofuran **3aa** in good yield (54%) employing only a slight excess of **1** (1.2 equivalents) and MeCN/H_2O (1/4) as the reaction medium (entry 1). However, although **3aa** was the major product, three other species were detected: the brominated hemiketal **4aa**, the lactone **5aa** and the hemiketal **6aa**.

According to published literature, we supposed that the formation of lactone **5aa** and hemiketal **6aa** was due to the presence of water.[33,38] Therefore, to minimize their formation, we tried the reaction in pure organic solvents (entries 2–3) but the transformation did not proceed. Assuming that water could confine the generated hydrobromic acid,[39] we repeated the reactions in organic solvents in the presence of 2,6-lutidine as base (entries 4–5), however the conversion remained very low. We concluded that $Ru(bpy)_3Cl_2$ required water to efficiently act as photocatalyst in this process, maybe not only to increase its solubility, but also due to a proton-coupled electron transfer (PCET) in which water acts as hydrogen bond donor.[34,40] Still, under these conditions the formation of side-products **5aa** and **6aa** was unavoidable.

Table 1. Reaction conditions optimization study.

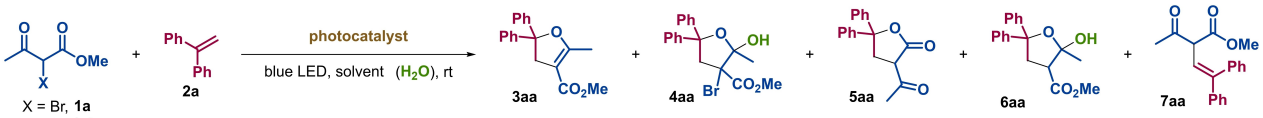

Entry	1 (X)	Photocatalyst	Solvent	Conversion (%)[a]	Yield (%)[b]				
					3aa	**4aa**	**5aa**	**6aa**	**7aa**
1	**1a** (Br)	$Ru(bpy)_3Cl_2$ $6H_2O$	MeCN/H_2O (1/4)	90	54	8	18	10	–
2		$Ru(bpy)_3Cl_2$ $6H_2O$	MeCN	< 10	nd	nd	nd	nd	nd
3		$Ru(bpy)_3Cl_2$ $6H_2O$	DMF	< 5	nd	nd	nd	nd	nd
4		$Ru(bpy)_3Cl_2$ $6H_2O$	MeCN	< 5	nd	nd	nd	nd	nd
5		$Ru(bpy)_3Cl_2$ $6H_2O$	DMF[c]	< 5	nd	nd	nd	nd	nd
6	**1a′** (Cl)	$Ru(bpy)_3Cl_2$ $6H_2O$	MeCN/H_2O (1/4)	< 5	nd	nd	nd	nd	nd
7		*fac*-Ir(ppy)$_3$	MeCN/H_2O (1/4)	100	22	–	18	44	–
8		*fac*-Ir(ppy)$_3$	MeCN	23	9	–	–	–	–
9		*fac*-Ir(ppy)$_3$	MeCN[c]	100	59	–	–	–	13
10		*fac*-Ir(ppy)$_3$	MeCN[c,d]	100	44	–	–	–	6
11		*fac*-Ir(ppy)$_3$	MeCN[c,e]	100	61	–	–	–	14
12		*fac*-Ir(ppy)$_3$	MeCN[c,f]	90	53	–	–	–	18
13		$Ir[dF(CF_3)ppy]_2(dtbbpy)PF_6$	MeCN[c]	< 5	nd	nd	nd	nd	nd
14		Eosin Y	MeCN[c,g]	< 5	nd	nd	nd	nd	nd
15		3DPA2FBN[h]	MeCN[c]	< 5	nd	nd	nd	nd	nd
16		Coumarin[h,i]	MeCN[c]	20	–	–	–	–	–

Reaction conditions: **1** (1.2 eq.), **2a** (0.1 mmol), photocatalyst (1 mol%), solvent (1 mL), blue LED (465 nm), freeze pump thaw (1 cycle), rt, 24 h.

[a] Determined by ^{1}H NMR spectroscopic analysis of the crude mixture using triphenylmethane as internal standard and integrating the signals of remaining reagent **2a**.

[b] Determined by ^{1}H NMR spectroscopic analysis of the crude mixture using triphenylmethane as internal standard and integrating the signals of the products.

[c] 2,6-Lutidine (1 eq.) was added.

[d] 2 mL of solvent.

[e] 2 eq. of **1a'**.

[f] 2 eq. of **2a**.

[g] Green LED (520 nm).

[h] 3 mol%.

[i] For the structure of employed coumarin see ref. [45]. rt = room temperature, bpy = 2,2′-bipyridine, ppy = 2-phenylpyridinato, dtbbpy = 4,4′-di-tert-butyl-2,2′-dipyridyl, DPA = diphenylamine, 2FBN = 3,5-difluoro benzonitrile, DMF = *N*,*N*-dimethylformamide, nd = not determined.

The brominated hemiketal **4aa** derived from methyl 2,2-dibromo-3-oxobutanoate always present in a certain percentage in substrate **1a**. Indeed, methyl 2-bromo-3-oxobutanoate **1a** (like many other bromoacetoacetates) is not commercially available and its synthesis provides a mixture of mono- and di-bromo derivatives, which are extremely difficult to be separated.[41] Moreover, **1a** proved to be not fully stable over time.[41] For all these reasons, we decided to move on to chlorinated analogues, many of which are stable and commercially available or easily synthesized. The relatively low oxidation potential of the excited photocatalyst $Ru(bpy)_3Cl_2$ ($E_{1/2}^{III/II*} = -0.81$ V *vs* SCE)[42] required the use of bromoacetoacetates, as the reaction did not take place with methyl 2-chloro-3-oxobutanoate **1a′** (entry 6). Therefore, we turned our attention to the more reducing photocatalyst *fac*-$Ir(ppy)_3$ ($E_{1/2}^{IV/III*} = -1.73$ V *vs* SCE),[42] which used under the conditions optimized for $Ru(bpy)_3Cl_2$ provided a mixture of three products (entry 7), where hemiketal **6aa** was the major one (44%). Aiming to increase the dihydrofuran **3aa** yield by reducing both lactone **5aa** and hemiketal **6aa**, we carried out the reaction in pure MeCN with and without base (entry 9 and 8, respectively). The disappearance of both the side-products confirmed that their formation was favored by water. High conversion and good yield (59%) of **3aa** were obtained only in the presence of a base (entry 9), although accompanied by a certain amount (13%) of β,γ-unsaturated β-ketoester **7aa**. To optimize the conditions we diluted the reaction mixture (entry 10) or increased the reactants quantity (**1a′**: entry 11, **2a**: entry 12, respectively), but significant improvements were not observed. The solvents screening (see Supporting Information) confirmed pure MeCN as the best reaction medium. Lastly, we carried out a brief photocatalysts screening. As expected, $Ir[dF(CF_3)ppy]_2(dtbbpy)PF_6$ ($E_{1/2}^{IV/III*} = -0.89$ V *vs* SCE)[42] was unable to promote the reaction (entry 13). Some organic photocatalysts were also tested. Eosin Y [E^*_{ox} ($cat^{\bullet+}$/cat*) = −1.15 V *vs* SCE][43] (entry 14), 3DPA2FBN [E^*_{ox} ($cat^{\bullet+}$/cat*) = −1.60 V *vs* SCE][44] (entry 15), and a highly reducing coumarin recently proposed by Cozzi *et al.* [E^*_{ox} ($cat^{\bullet+}$/cat*) = −1.89 V *vs* SCE][45] (entry 16) were not able to promote the dihydrofuran formation. Our optimization study continued by investigating the reaction time (see Supporting Information) and 24 hours was identified as the best one. Since we observed a significant role of the base in this process (Table 1, entries 8–9), we investigated the effect of base equivalents on **3aa** formation (see Supporting Information). The best performance with the model substrates was achieved with stoichiometric base, whereas an excess did not improve the reaction outcome. At last, the nature of the base was studied (see Supporting Information). Some organic bases showed low conversions, others provided high conversions but many by-products. The optimal result was obtained with the inorganic base Na_2HPO_4, that promoted a very clean reaction furnishing the dihydrofuran **3aa** in 84% yield.

Reaction scope and chemodivergence. With the optimized conditions in our hands, we turned our attention to the reaction scope and different olefins **2** were employed (Scheme 2).

Several substituted 1,1-diarylethylenes **2b–f** were tested. When only one aromatic ring was substituted, both electron-donating (**3ab** and **3ac**) and electron-withdrawing (**3ad**) groups were well tolerated, in *ortho* e *para* positions. When the two aromatic rings were both substituted, electron-withdrawing groups (EWGs) were tolerated but the process slowed down (**3ae**).[46] Differently, two electron-donating groups (EDGs) (**3af**) influenced the reactivity to the point of triggering the formation of a remarkable amount (37%) of β,γ-unsaturated β-ketoester **7af**. As observed also by other authors,[16,35c] very electron-rich aromatic rings favor the formation of the conjugated double bond. It is noteworthy that aryl chlorides remained untouched

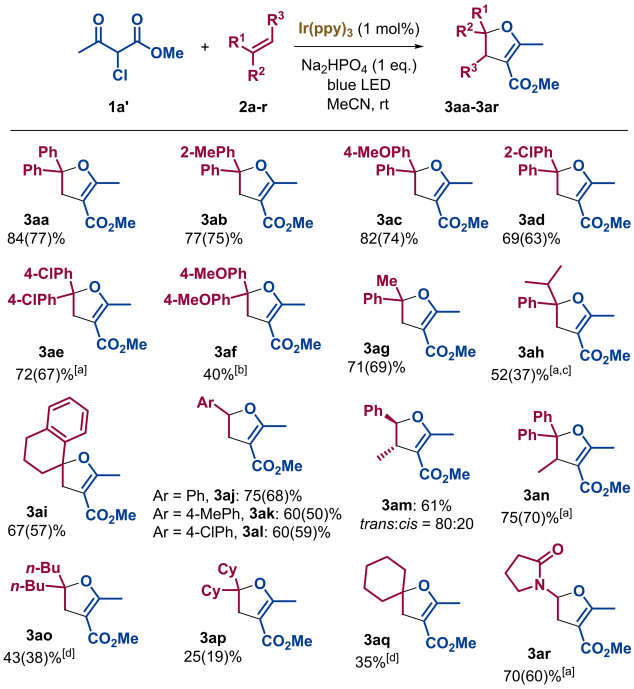

Scheme 2. Alkenes **2** scope. Optimized reaction conditions: **1a′** (1.2 eq.), **2** (0.1 mmol), $Ir(ppy)_3$ (1 mol%), Na_2HPO_4 (1 eq.), MeCN (1 mL), blue LED (465 nm), freeze pump thaw (1 cycle), rt, 24 h. All the products were obtained as racemates. NMR yields determined by ^{1}H NMR spectroscopic analysis of the crude mixture using triphenylmethane as internal standard and integrating the signals of the products. Yields after flash chromatography reported in brackets. [a] Reaction time: 72 h. [b]37% (NMR yield) of product **7af** was also detected. The two products were inseparable. [c]46% (NMR yield) of lactone **5ah** was also detected. [d] 2.5 eq. of alkene.

(**3 ad**, **3 ae** and **3 al**), demonstrating the orthogonality between these photoredox conditions and the classic transition metal-based protocols. The presence of aryl chlorides allows later stage functionalizations. We proceeded with the evaluation of 1-alkyl-1-arylethylenes **2 g–i**, which successfully provided the corresponding dihydrofurans **3 ag–3 ah** and the structurally ambitious spiro compound **3 ai**. However, we observed that the steric hindrance present on the olefin significantly affects the reaction outcome,[46] as demonstrated by 1-isopropyl-1-phenylethylene **2 h**, which reacted slowly and also generated the corresponding lactone **5 ah** (46%) (see Supporting Information for our hypothesis on **5 ah** formation). Particularly worthmentioning were the results obtained with the variously substituted styrenes **2 j–l**, which furnished the corresponding dihydrofurans **3 aj–3 al** in good yields without significant formation of the corresponding furans, thanks to the mild and redox-neutral reaction conditions. 4-Nitro styrene was also tested but no reaction took place, probably because this alkene is too electron-poor. The developed method was successfully applied to 1,2-disubstituted olefin **2 m** providing the corresponding dihydrofuran **3 am** preferentially as *trans*-isomer.[16,37,47] Lastly, we tested the trisubstituted alkene **2 n** and, although the reaction took longer, the crowded dihydrofuran **3 an** was obtained in good yield (75%). At this point we turned our attention to 1,1-dialkylethylenes, which are unable to provide stabilized benzylic radical and/or cationic intermediates. Dibutylethylene **2 o** furnished dihydrofuran **3 ao** in acceptable yield (43%), however the results obtained from dialkyl olefins (**2 o–q**) were generally worse. This behavior was confirmed by the comparison between products **3 ai** and **3 aq**: in both cases we observed the formation of the spiro compound, but the yield doubled in the presence of an aromatic substituent on the olefin (**3 ai**). Also using 1,1-dialkylethylenes, the increase of steric hindrance reduced the reaction efficiency (**3 ao** *vs* **3 ap**). Moreover, we subjected 1-decene to our reaction conditions, as an example of monosubstituted aliphatic alkene. However, a complex mixture of different products was obtained. We concluded the olefins investigation employing 1-vinyl-2-pyrrolidinone **2 r** as heteroatom-substituted alkene, which provided the desired dihydrofuran **3 ar** in good yield (70%). There is only one previous synthesis of dihydrofurans with an analogous substitution pattern, based on the use of α-diazoesters with rhodium(II)-catalysis.[48] Moreover, it is interesting to underline that Zhang and Yu applied an iridium-based photocatalytic protocol to 1-vinyl-2-pyrrolidinone **2 r** in the presence of α-bromo β-ketoesters and they obtained exclusively the corresponding β,γ- (or α,β-) unsaturated derivatives.[49]

Afterwards, we turned our attention to the reactivity of various α-haloketones **1** (Scheme 3). Based on the good results obtained with methyl 2-chloro-3-oxobutanoate **1 a'** (product **3 aa**, Scheme 3 – ***Chart A***), we tested some differently substituted chlorinated β-ketoesters (**1 b–c**). Dihydrofuran **3 ba** was isolated in excellent yield (86%) starting from substrate **1 b** characterized by an aromatic ketone. This result is remarkable because many authors reported that under similar conditions aromatic ketones preferentially generate α-tetralones or 1-naphthols, resulting from the addition of an intermediate (cationic or radical) to the

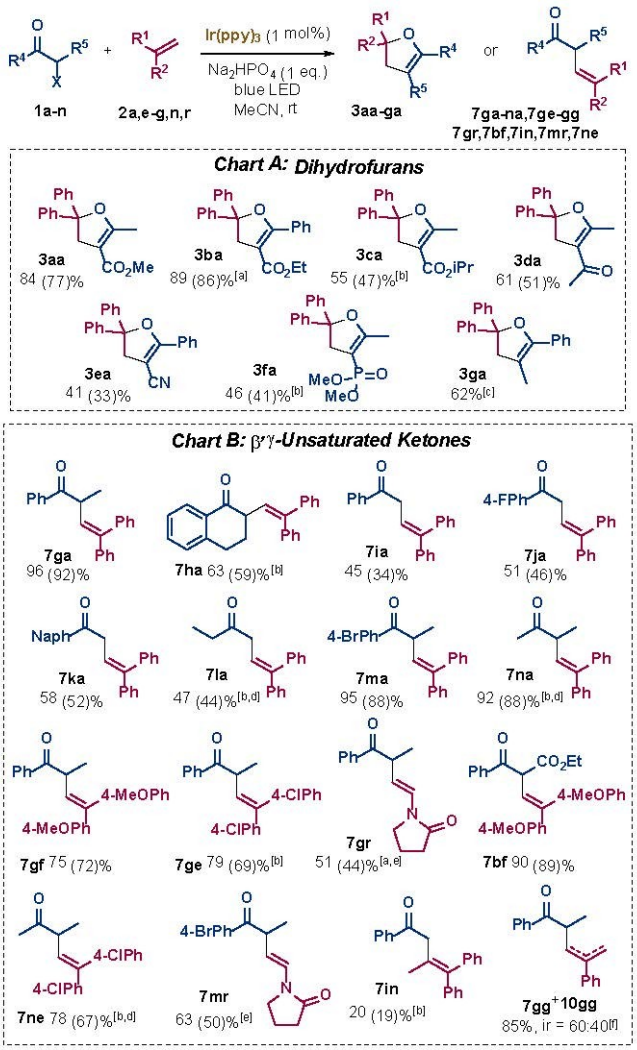

Scheme 3. α-Haloketones **1** scope. For optimized reaction conditions see Scheme 2. NMR yields determined by ^{1}H NMR spectroscopic analysis of the crude mixture using triphenylmethane as internal standard and integrating the signals of the products. Yields after flash chromatography reported in brackets. [a] Reaction time: 48 h. [b] Reaction time: 72 h. [c] 19% (NMR yield) of product **7 ga** was also detected. Yield after flash chromatography of **3 ga** was not given due to its conversion to **7 ga** on silica gel. [d] 2.5 eq. of **1**. [e]2.5 eq. of **2**. [f] ir = isomeric ratio; the major isomer **7 gg** is characterized by the trisubstituted double bond.

phenyl ring.[35a,50] As demonstrated by the good yields of products **3aa** and **3ba**, methyl and ethyl esters were both well tolerated. However, the increase of steric hindrance on the ester portion reduced the reactivity,[51] as the isopropyl derivative **1c** reacted more slowly, furnishing the dihydrofuran **3ca** in acceptable but lower yield (55%). We proceeded replacing the ester group with other functional groups, such as ketone (**1d**) or nitrile (**1e**). The 1,3-diketone **1d** worked fairly under our reaction conditions (product **3da**, Scheme 3 – ***Chart A***). Conversely, 2-chloro-3-oxo-3-phenylpropanenitrile **1e** provided the corresponding dihydrofuran **3ea** with lower conversion and yield.[16] We also tested the reactivity of dimethyl 1-chloro-2-oxopropylphosphonate (**1f**), bearing a less conventional EWG at α-position. It proved to be not very reactive, however it cleanly generated dihydrofuran **3fa** in acceptable yield (46%).[52] 4-Phosphonyl-2,3-dihydrofurans can be exploited as synthetic precursors of antiviral compounds.[53] Lastly, we applied our protocol to 2-chloro-2-nitro-1-phenylethan-1-one characterized by a nitro substituent as EWG at α-position. However, we observed a low olefin conversion and the formation of different unidentified products.

Afterwards, we turned our attention to α-haloketones lacking EWGs at α-position. 2-Chloro-1-phenyl-1-propanone **1g'** provided dihydrofuran **3ga** in good yield (62%, Scheme 3 – ***Chart A***), but a considerable amount (19%) of β,γ-unsaturated product **7ga** was also detected. Conversely, starting from cyclic ketone 2-chlorotetralone **1h** we isolated the corresponding α-alkenylation derivative **7ha** as the only reaction product (Scheme 3 – ***Chart B***). Further similar unexpected results were provided by 2-chloroacetophenone **1i'** and 2-chloro-4-fluoro acetophenone **1j**, which, unlike the propyl analogue **1g'**, furnished the corresponding β,γ-alkenyl ketones **7ia** and **7ja** as the only reaction products, even if in moderate yields (32% and 51% respectively; Scheme 3 – ***Chart B***). In these latter cases, the low process efficiency was probably due to the formation of a relatively unstable primary alkyl radical intermediate, as observed also by other authors.[54]

At this point, we were curious about the behavior of bromoketones under our optimized conditions. From methyl 2-bromo-3-oxobutanoate **1a** we obtained the expected dihydrofuran **3aa** with a much lower yield (31%) than the corresponding chlorinated β-ketoester **1a'** (84%), being present in the crude mixture the β,γ-alkenyl derivative **7aa** (18%) and other unidentified species. However, the most intriguing result was recorded with 2-bromo-1-phenyl-1-propanone **1g** generating the β,γ-unsaturated product **7ga** with quantitative yield (96%, Scheme 3 – ***Chart B***), whereas its chlorinated analogue **1g'** preferentially provided dihydrofuran **3ga** (62%, Scheme 3 – ***Chart A***). The different products distribution (**3** *vs* **7**) obtained under the same reaction conditions and with the same olefin by varying only the halogen present in the ketone (Cl in **1g'** *vs* Br in **1g**, respectively) is difficult to be rationalized and, in the vast majority of cases, the halogen role is not explored in depth when new photoredox processes are proposed. Nevertheless, Yoon has recently demonstrated that the counterion can exert a remarkable impact on the observed rate of radical reactions promoted by photoredox catalysts.[55] Usually, the chemoselectivity between dihydrofuran and β,γ-unsaturated ketone formation was described as dependent on the solvent,[9a,50b,56] the metal oxidant[57] or on the additive.[58] However, Lei observed that different halides have distinct effects on the copper-mediated redox processes leading to dihydrofurans.[13c,59] In our photocatalytic transformation, the employed halide might affect several reaction steps, starting from the reduction of the α-haloketone operated by the excited *fac*-Ir(ppy)$_3$ and the oxidation of the radical intermediate to carbocation operated by the [Ir(IV)]X species. Different kinetics of these steps, due to the halogen variation, could favor different reaction pathways. Furthermore, the oxidation of the radical intermediate by the [Ir(IV)]X species provides a carbocation pre-associated with the halide,[60] with the nucleophilicity parameters suggesting a favored trapping for bromide with respect to chloride (13.8 for bromide, 12.0 for chloride).[61] Moreover, in the case of α-bromo-ketones and -ketoesters, we cannot completely exclude a contribute due to the abstraction of a bromo-radical from the reagent by the generated radical intermediate.[54a,62] Lastly, the halide (especially in the case of bromide) might not to be fully innocent in the reaction mixture due to its redox properties.[33]

In order to obtain β,γ-alkenyl ketones **7** in good to excellent yields, we decided to exploit our photocatalytic protocol as new strategy for the α-alkenylation of carbonyl substrates. In particular, a process able to provide β,γ-alkenyl ketones avoiding the intrinsic limitation of their rearrangement into the α,β-unsaturated[49] is highly desirable. The β,γ-alkenyl ketone motif is present in several natural bioactive compounds (Figure 2)[63] and the further manipulations possible on these scaffolds make them very attractive as synthetic intermediates.[64]

For these reasons the synthesis of β,γ-alkenyl ketones has aroused great interest in the last decades. The α-alkenylation of carbonyl substrates is the most employed and synthetically useful approach to achieve these products and two are the main strategies: a) the addition of enolates to terminal alkynes[64g,65] or halogenated olefins;[66] b) the coupling between α-haloketones and terminal alkynes.[50c,67] The vast majority of the published procedures using unfunctionalized olefins works on α-halo-esters, -amides or -active methylene compounds.[49,54a,68] Very few examples describe the direct α-alkenylation of α-haloketones

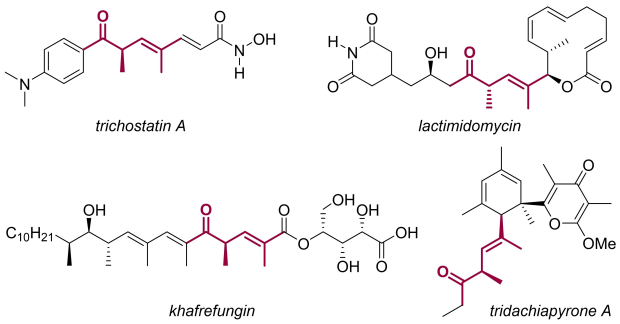

Figure 2. A selection of bioactive compounds containing the β,γ-alkenyl ketone moiety.

by reaction with unactivated olefins[69] and all these protocols were developed for different substrates, being the ketone mentioned as single example. Moreover, only fully α-substituted carbonyls were used to avoid the product rearrangement to α,β-unsaturated derivative. On this basis, we developed the first photoredox catalytic coupling between α-haloketones and unfunctionalized olefins providing variably substituted β,γ-alkenyl ketones in good yields. Different α-haloketones (**1 g–n**) were tested with 1,1-diphenylethylene **2 a** and all the substrates selectively furnished the corresponding β,γ-alkenyl ketones **7** as the only reaction product (Scheme 3 – ***Chart B***). Starting from the aceto-derivatives (**1 i–l**) the yields were around 50% (products **7 ia–7 la**), probably due to the primary radical intermediate, as already mentioned. However, exactly for this reason, these results are valuable. In fact, many radical alkenylation protocols do not work on α-halo aceto-derivatives.[35b,67a,68a] As expected, we achieved superior yields (92–96%, products **7 ga, 7 ma, 7 na**) with α-methyl α-bromoketones (**1 g, 1 m–n**), bearing both aliphatic or aromatic substituents. Aiming to expand our library of β,γ-alkenyl ketones **7**, we reacted some α-bromoketones with different olefins obtaining the expected products in good yields (**7 ge**, **7 gf**, **7 gr**, **7 ne** and **7 mr**). α-Methylstyrene **2 g** provided high conversion, however, the β,γ-alkenyl ketone **7 gg** was obtained in mixture with the γ,δ-alkenyl ketone **10 gg**. The trisubstituted alkene **2 n** was also tested: the reaction with 2-bromo-1-phenyl-1-propanone **1 g** did not proceed, whereas 2-bromoacetophenone **1 i** furnished the expected product **7 in** although in low yield. These findings confirm a significant impact of the steric hindrance on the radical addition to the olefin. We proceeded by reacting 2-bromo-1-phenyl-1-propanone **1 g** with two different 1,1-dialkylethylenes. In the presence of 1,1-dicyclohexylethylene **2 p** the transformation did not take place even after 72 hours. Conversely, a peculiar behavior was shown by 1,1-dibutylethylene **2 o** providing the corresponding substituted tetralone as the main reaction product (53%) (see Supporting Information). Lastly, we confirmed the already observed (Scheme 2) peculiar behavior of 1,1-di-*p*-methoxyphenylethylene **2 f**, which allowed us to quantitatively obtain the α-alkenylation product **7 bf** starting from chloro β-ketoester **1 b** (Scheme 3 – ***Chart B***).

By analyzing in details our products library (Schemes 2 and 3), it was clear that several characteristics of the starting materials affected the efficiency and, more importantly, the products distribution of our photocatalytic radical process (Scheme 4). We observed that the electronic properties of the ketone α-substituent (R^5) played a crucial role. EWGs as ester (**1 a–c**), ketone (**1 d**), nitrile (**1 e**), and phosphonate (**1 f**) preferentially led to dihydrofurans **3**. Conversely, unsubstituted (**1 i–l**) or alkyl-substituted (**1 g–h**, **1 m–n**) α-haloketones preferentially provided the corresponding β,γ-alkenyl derivatives **7**. As previously mentioned, the employed halogen (X) seemed to have a slight influence on the reaction outcome, with bromine favoring the α-alkenylation product compared to chlorine (**1 g** *vs* **1 g'**, products **7 ga** *vs* **3 ga**, respectively).

Concerning the group directly linked to the carbonyl (R^4), alkyl- and aryl-substituents were both well tolerated in the synthesis of both dihydrofurans **3** and β,γ-alkenyl ketones **7**. However, in the case of cyclic α-chloro ketones, we obtained a good reactivity with α-chloro tetralone **1 h** (63% yield of **7 ha**; Scheme 3 – ***Chart B***), whereas α-chloro cyclohexanone **1 s** showed a much lower reactivity (only 13% of **2 a** consumption after 24 h; data not shown). These findings highlighted a superior reactivity of cyclic aromatic ketones (R^4 = Ar) with respect to cyclic aliphatic ketones (R^4 = Alk). Lastly, it was evident that the olefin substituents (R^1 and R^2) had a remarkable role in directing the transformation towards **3** or **7**. It was already reported that the alkene electronic effects significantly affect the outcome of similar transformations[35c] and some authors justified their results considering that electron-donor substituents favor the radical oxidation[70] and the following double bond formation. Our results aligned with those already

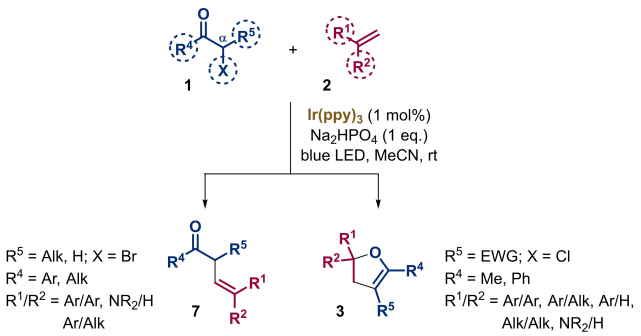

Scheme 4. Substrate-dependent chemodivergent transformation.

reported. Although a single EDG was tolerated (**3 ab** and **3 ac**, Scheme 2), two EDGs on the olefin (**2 f**) triggered the formation of a considerable amount of β,γ-unsaturated ketone (37% of **7 af**). Moreover, a quantitative α-alkenylation was obtained reacting β-ketoester **1 b** with this highly electron-rich olefin (**2 f**), whereas the same β-ketoester provided only dihydrofuran when reacted with less electron-rich 1,1-diphenylethylene **2 a** (**7 bf** *vs* **3 ba**, respectively).

As last remark, we applied our photocatalytic protocol to α,α-disubstituted α-haloketones **1 o–r** (Scheme 5). With these compounds the final proton-elimination leading to dihydrofurans **3** was not possible, therefore, we expected the formation of the corresponding β,γ-alkenyl derivatives **7**, as experimentally observed by many authors.[49,51,68d,69] Conversely, all the tested quaternary α-haloketones subjected to our reaction conditions generated the cyclic hemiketal **6** as the only reaction product, characterized by a tetrahydrofuran skeleton with three quaternary carbons (Scheme 5).

These highly substituted cyclopentyl hemiketals (**6**) are useful synthetic intermediates,[71] in particular for the preparation of materials[72] and medicinally relevant molecules.[73] Our approach represents a particularly straightforward synthesis of these scaffolds, which were obtained for the first time in high yield by radical addition of ketones to olefins.[74] Among the obtained compounds, 2-acetyl-2-chlorocyclohexan-1-one **1 o** provided the spiro product **6 oa** in good yield (56%) as single diastereoisomer, and 2-chloro-2,2-difluoroacetophenone **1 r** quantitatively furnished the fluorinated hemiketal **6 ra**. Only Konno and co-workers obtained products with a similar substituents distribution but exploiting a much longer synthetic pathway.[72,75]

Supposing a significant role of water in the formation of these compounds, we repeated the synthesis of **6 qa** in MeCN/H_2O mixture and we gratifyingly obtained the desired product in quantitative yield (93%). In general, the reactions involving these substrates (**1 o–q**) were slow (72 hours), probably because the steric hindrance around the radical carbon slowed the addition to the olefin. However, we observed a higher reactivity for α-EWG-substituted ketones (**1 o**, **1 p** and **1 r** *vs* **1 q**), which could generate more electrophilic and reactive radicals.

Mechanistic investigations. The study of processes involving oxidation states modifications is known to be a challenging task, due to the formation of reactive intermediates with short life-times.[76] To better understand the reaction mechanism of our photoredox Ir-catalysed transformations, we decided to set up some properly designed experiments and to confirm the existence of the proposed intermediates with DFT calculations.

First, were carried out a series of reactions in different conditions, to demonstrate the visible light-promoted radical pathway of our reaction (Table 2). The crucial role of both the photocatalyst and light was confirmed, since in their absence the reactants were completely unreactive (entries 2–3, Table 2). A prominent role for the excited photocatalyst *fac*-Ir(ppy)$_3$ as initiator of a radical chain propagation mechanism was also excluded. In fact, the overall amount of cyclic products (**3 aa** + **6 aa**) obtained after two hours of irradiation (entry 4) almost exactly matched with the yield of the product **3 aa** obtained after 22 hours of further stirring in the dark (entry 5, see Supporting Information for a detailed study). Moreover, the measured photoreaction quantum yield was 0.24, reasonably confirming a closed catalytic cycle ($\Phi < 1$) and ruling out a radical chain propagation mechanism (see Supporting Information for details).[33b] The radical inhibitor TEMPO completely stopped the reaction (entry 6), thus suggesting an electron transfer-triggered radical pathway. Furthermore, a high resolution mass spectrometry (HRMS) study allowed us to

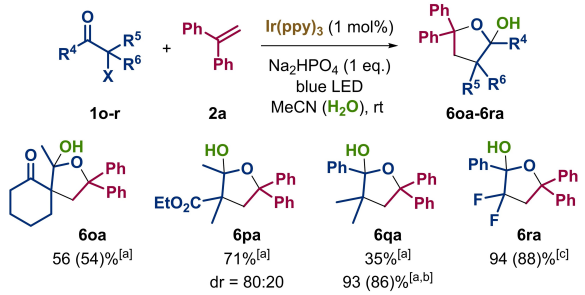

Scheme 5. For optimized reaction conditions see Scheme 2. NMR yields determined by ^{1}H NMR spectroscopic analysis of the crude mixture using triphenylmethane as internal standard and integrating the signals of the products. Yields after flash chromatography reported in brackets. [a] Reaction time: 72 h. [b] The mixture MeCN/H_2O (1/4) was used as solvent without base. [c] Reaction time: 24 h.

Table 2. Investigations on the reaction mechanism.

Entry	Reaction conditions modification	t [h]	Yield [%][b] **3 aa**	**6 aa**	**7 aa**
1	–[a]	24	84	–	–
2	No catalyst	24	–	–	–
3	No light	24	–	–	–
4	–	2	12	4	–
5	Light + dark	2 + 22	17	–	–
6	TEMPO (2 eq.)	24	–	–	–
7	No freeze pump thaw	24	46	–	10

[a] For optimized reaction conditions see Scheme 2. [b] Determined by ^{1}H NMR spectroscopic analysis of the crude mixture using triphenylmethane as internal standard and integrating the signals of the products. TEMPO = 2,2,6,6-tetramethylpiperidine-1-oxyl.

detect the adduct between TEMPO and β-ketoester, supposed to generate the first radical intermediate (see Supporting Information for details). At last, we proved that the presence of oxygen, a well-known quencher of the excited state of many transition-metal polypyridyl compounds,[77] actually made the transformation less efficient, providing dihydrofuran **3aa** in lower yield (46%) together with some by-products (entry 7).

Second, Stern-Volmer luminescence quenching experiments (see Supporting Information) demonstrated that the quenching of excited *fac*-Ir(ppy)$_3$ was accomplished by the α-chloro substrate **1a′**, supporting the postulated SET in generating the first α-keto radical intermediate.

Finally, to evaluate the possible occurrence of an atom-transfer reaction eventually followed by the elimination of HX, we analyzed by ^{1}H-NMR, GC-MS and HRMS the crude mixtures deriving from ketoester **1a′** and ketone **1g**. No organic halide had ever been detected, even in the absence of base or in the presence of an excess of LiCl as carbocation quencher[60,62] (see Supporting Information for details). These findings might suggest that the atom-transfer does not occur. However, the reaction of the intermediate halide might be so fast that it cannot be detected.

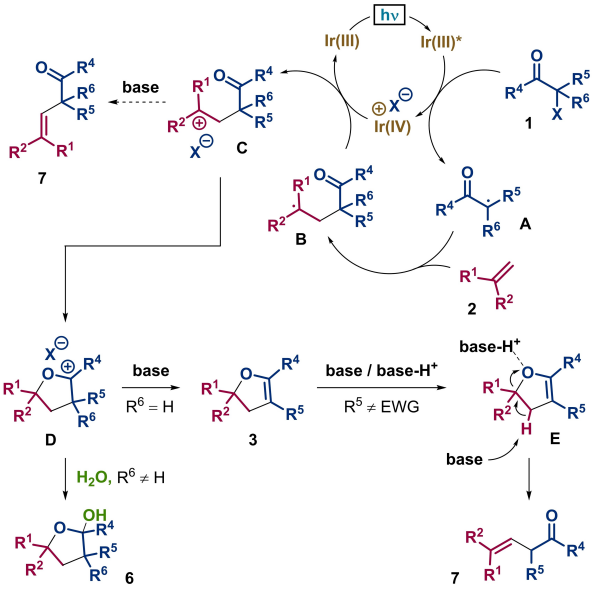

Scheme 6. Polar cyclization pathway.

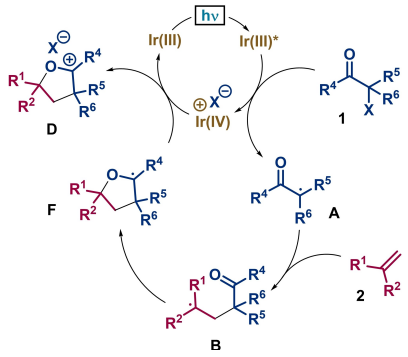

Scheme 7. Radical cyclization pathway.

Based on the experimental evidences so far obtained and on previous literature reports, a reasonable mechanistic rationale for our photoredox Ir-catalyzed transformation was formulated, as shown in Schemes 6 and 7. Under visible light irradiation, $Ir^{III}(ppy)_3$ is photoexcited to $[Ir^{III}(ppy)_3]^*$ ($E_{1/2}^{IV/III*} = -1.73$ V),[42] which undergoes a single electron transfer (SET) process in the presence of α-halo ketone **1**,[78] generating $Ir(IV)^+X^-$ species and the electrophilic radical **A**. This intermediate adds to electron-rich olefin **2** providing radical **B**, which, in principle, can follow two different reaction pathways (Schemes 6 and 7). In the first possible path (Scheme 6), radical **B** is oxidized ($E_{1/2}^{ox} = +0.23$ V *vs* SCE for **2a** and **2n**, $E_{1/2}^{ox} = +0.16$ V *vs* SCE for **2g**, $E_{1/2}^{ox} = +0.37$ V *vs* SCE for **2j** and **2m**, $E_{1/2}^{ox} = +0.09$ V *vs* SCE for **2o**)[79] by Ir(IV) species ($E_{1/2}^{IV/III} = +0.77$ V),[42] restoring the Ir(III)-complex and generating carbocation **C**. This highly reactive intermediate may directly afford product **7** by base-promoted elimination, or may undergo a *polar cyclization* providing the cyclic cationic intermediate **D**. This species differently behaves depending on the substitution pattern. When a hydrogen is present at α-position of the ketone (R^6 = H), the reactive intermediate **D** preferentially evolves through a base-assisted proton-elimination leading to dihydrofuran **3**. Conversely, if no hydrogen is present at the α-position (R^6 ≠ H), hemiketal **6** is formed by interception of cation **D** by traces of water present in the reaction mixture. Indeed, the generation of hemiketal **6** is increased in the presence of a large amount of water as a reagent (entry 7, Table 1; product **6qa**, Scheme 5).

Concerning dihydrofurans **3**, we observed a completely different stability depending on the electronic properties of the substituent R^5, in particular under slightly acidic conditions. Stable dihydrofurans are obtained starting from ketones **1** substituted at the α-position with EWGs, while the methyl-substituted dihydrofuran **3ga** converted spontaneously to the β,γ-unsaturated ketone **7ga** over silica gel or in $CDCl_3$. These experimental findings led us to postulate that the β,γ-unsaturated ketones **7** were formed from the corresponding dihydrofurans **3**, through an acid-mediated oxygen protonation followed by ring-opening and proton-elimination (Scheme 6).[48,51,58,80] This hypothesis was also supported by separate experiments conducted by treating the obtained dihydrofurans **3** with the acidic species generated during the reaction (see Supporting Information for details).

Although the most popular mechanisms invoked for similar radical transformations support almost com-

pletely the above mentioned mechanistic rationale (Scheme 6), we cannot completely rule out the possibility of a *radical cyclization* pathway, as reported in Scheme 7. In this second possible path, radical **B** directly cyclizes, providing the oxygen-substituted radical **F**, which in turn is oxidized by $Ir(IV)^+X^-$ species ($E_{1/2}^{IV/III} = +0.77$ V).[42] According to a radical-polar crossover transformation, the $Ir^{III}(ppy)_3$ photocatalyst would be regenerated by oxidation of radical **F** to carbocation **D**, which then evolves as already described (Scheme 6). However, the oxidation of oxygenated radical **F** should be less favored than the oxidation of radical **B**.[79b,81] Many papers report both mechanisms (polar and radical cyclizations) as possible,[8c,15,16,34,52c] and some authors believe the radical cyclization to be more likely under certain reaction conditions.[13c,17,25b,38,50e,57,82] Aiming to learn more about the mechanism of our photocatalytic process, we performed some DFT computational investigations comparing the *polar cyclization* (Scheme 6) and the *radical cyclization* (Scheme 7) pathways. Moreover, we also tried to get a deeper insight on the chemodivergent behavior of α-EWG-substituted and α-unsubstituted/alkyl-substituted halo ketones **1**.

DFT calculations. Given the reasonable existence of the radical **A** in the postulated mechanism, we started by modeling the reaction of radical **Aa** (R^4 = Me, $R^5 = CO_2Me$, $R^6 = H$) deriving from **1a** or **1a'** with alkene **2a** in the presence of 2,6-lutidine as the base (Table 1, Entry 9, see Supporting Information for details). The complete calculated energy profile for this transformation at the M06-2X/6-31+G(d,p)//M06-2X/cc-pvtz using CH_3CN as the solvent, affording either **3aa** or **7aa**, is depicted in Figure 3. The initial radical addition to give intermediate **Ba** resulted in a very favorable exergonic reaction ($\Delta G_{298} = -21.7/-24.0$ kcal·mol^{-1}), characterized by a low-lying transition state (**TS1**, $\Delta G^{\neq} = 5.8/3.4$ kcal·mol^{-1}). On the contrary, the direct radical cyclization of **Ba** to afford **Fa** was a rather endergonic reaction ($\Delta G_{298} = 12.1/14.6$ kcal·mol^{-1}), with a considerably large activation energy (**TS2**, $\Delta G^{\neq} = 27.4/28.0$ kcal·mol^{-1}). To assess the feasibility of the oxidation reaction of radical **Ba** to the carbocation **Ca** by Ir(IV) species, the corresponding oxidation potential was calculated according to the procedure recently reported by Nicewicz,[78c] by fully optimizing the relevant structures at the M06-2X/6-31+G(d,p) and using CH_3CN as the solvent (see Supporting Information for details). The calculated oxidation potential ($E^{\circ}_{1/2} = +0.37$ V *vs* SCE, CH_3CN) was comparable with the values experimentally obtained for analogous benzhydryl derivatives[79] and it accounts for a thermodynamically favored oxidation reaction ($\Delta G_{298} = -24.9$ kcal·mol^{-1}). The so obtained carbocation **Ca** may now follow two distinct reaction

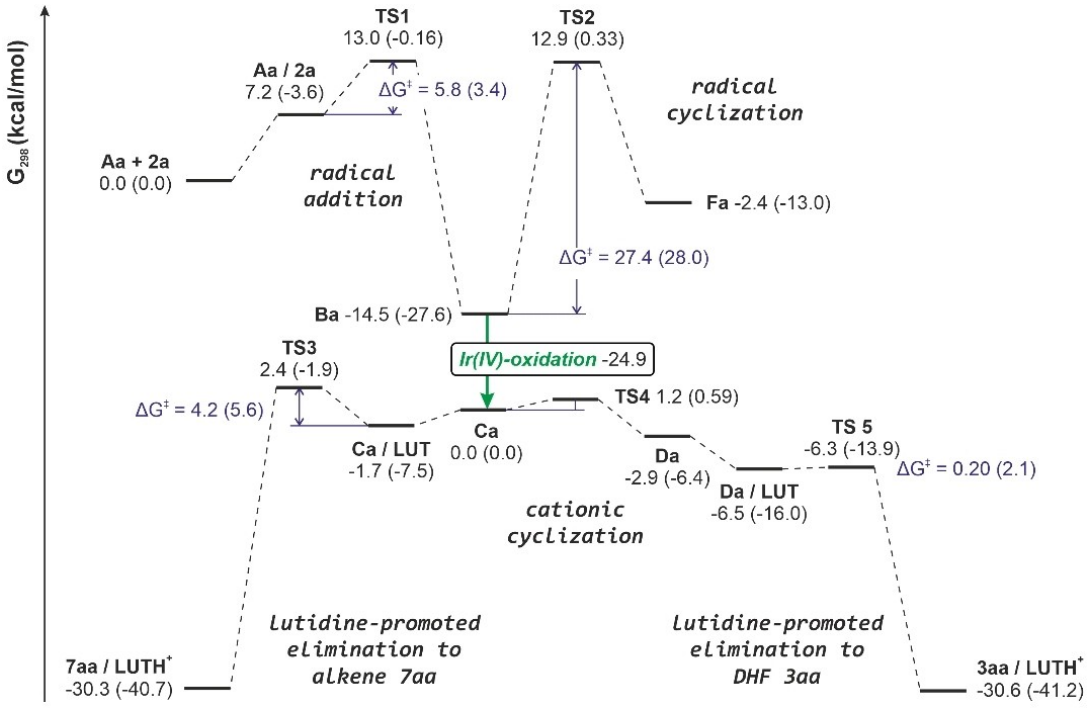

Figure 3. Complete free energy profile (kcal·mol^{-1}) for the reaction between radical **Aa** and olefin **2a** to afford alkene **7aa** or dihydrofuran (DHF) **3aa** in the gas-phase at the M06-2X/6-31+G(d,p) level of theory. Energies in parentheses are relative to single point calculations at the M06-2X/cc-pvtz level of theory in CH_3CN. **LUT** = 2,6-lutidine. Energies of **Ca**, **TS4** and **Da** are scaled by adding 2,6-lutidine calculated energy.

pathways, either a lutidine-promoted elimination to afford β,γ-unsaturated ketone **7aa** (Figure 3, bottom left) or a cationic cyclization to cation **Da**, followed again by a lutidine-promoted elimination to give the dihydrofuran **3aa** (Figure 3, bottom right). All involved reactions are favorable exergonic transformations with low activation energies. However, the cationic cyclization resulted slightly favored over the competing elimination reaction (**TS4/TS3**, $\Delta\Delta G^{\ddagger} = -1.2/-1.3$ kcal·mol^{-1}), qualitatively accounting for the experimentally obtained results (Table 1, Entry 9: **3aa**/**7aa** = 82/18), also considering that the subsequent elimination reaction to **3aa** via **TS5** resulted an almost barrierless transformation.

The analogous energy profile for the reaction of radical **Ag** (R^4 = Ph, R^5 = Me, R^6 = H) deriving from **1g**, a ketone lacking the EWG at the α-position, with alkene **2a** in the presence of 2,6-lutidine as the base is depicted in Figure 4. Given the similar oxidation potential value obtained also for the oxidation of radical **Bg** to cation **Cg** by Ir(IV) species, ($E^{\circ}_{1/2} = +0.31$ V *vs* SCE, CH_3CN; $\Delta G_{298} = -26.3$ kcal·mol^{-1}), the radical cyclization pathway was not calculated in this case and the cationic pathway was postulated to be once again the most favorable one. Even if some differences resulted by comparing the energy profiles relative to the reactions between **1a'** or **1g** with **2a** – most notably a true barrierless cationic cyclization in the case of **1g** and a larger elimination barrier both for **TS7** *vs* **TS3** and for **TS8** *vs* **TS5** – the two profiles were qualitatively similar. Once more, the formation of cyclic product **3ga** seems to be favored also in the case of ketone **1g**, contrary to what was experimentally found.

Summarizing the results of DFT calculations, Ir(IV) species are able to easily oxidize radicals **B** to the corresponding carbocations **C**, fostering a very favorable cationic cyclization pathway, ultimately leading to the formation of dihydrofurans **3**, excluding a relevant contribution of a direct elimination reaction in the formation of β,γ-unsaturated ketones **7** from cations **C** (Scheme 6). Moreover, the radical cyclization pathway (Scheme 7) resulted considerably more energetically demanding than the cationic one, therefore it probably doesn't play a relevant role in the overall reaction mechanism. Finally, DFT calculations confirmed that the chemodivergent behavior of ketones not possessing an EWG at the α-position is a direct consequence of the experimentally determined lower stability of the corresponding dihydrofurans **3**, rather than the result of a competing reaction pathway. According to our hypothesis (Scheme 6), we supposed that the protonated base present in the reaction mixture could act as an acid additive, triggering a base-assisted ring opening of the alkyl-substituted (or not substituted) dihydrofuran and promoting the formation of the observed

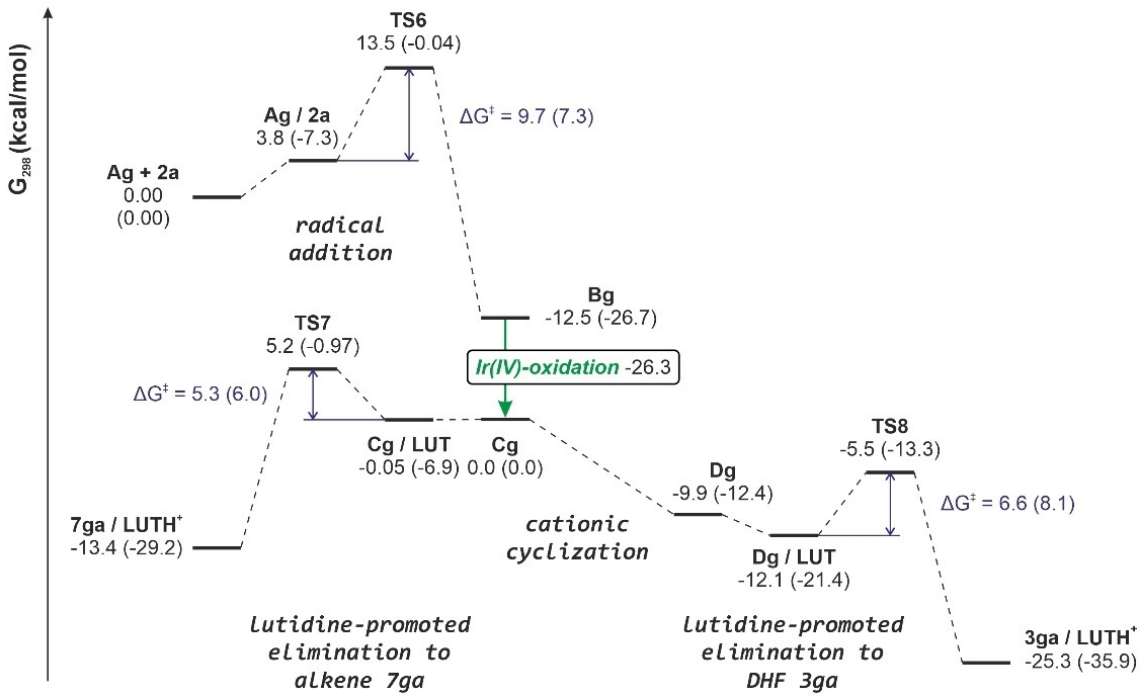

Figure 4. Complete free energy profile (kcal·mol^{-1}) for the reaction between radical **Ag** and olefin **2a** to afford alkene **7ga** or dihydrofuran (DHF) **3ga** in the gas-phase at the M06-2X/6-31+G(d,p) level of theory. Energies in parentheses are relative to single point calculations at the M06-2X/cc-pvtz level of theory in CH_3CN. **LUT** = 2,6-lutidine. Energies of **Cg** and **Dg** are scaled by adding 2,6-lutidine calculated energy.

alkenylation product **7**. This ring opening pathway may be less efficient in the presence of an EWG (R^5) both depleting the endocyclic oxygen of electron density and competing for the hydrogen-bonding with the protonated base. Confirming this last hypothesis, it is worth mentioning that the lutidinium cation in the final calculated structure **3ga/LUTH$^+$** moved considerably away from the initial deprotonation position, to bind the dihydrofuran endocyclic oxygen (Figure 5b), while it remained almost in the same position in the case of **3aa/LUTH$^+$**, stabilized by a hydrogen bond interaction with the ester moiety at the α-position (Figure 5a).

To further support this mechanistic hypothesis experimentally, we performed some reactions in the presence of two equivalents of 2,6-lutidine as a soluble base (Scheme 8).

By minimizing the enol oxygen protonation, the photocatalytic process furnished dihydrofurans **3** as the main products also starting from alkyl- or phenyl-substituted α-halo ketones **1**. These experimental findings, together with the results of DFT calculations, confirmed that in our reaction conditions β,γ-unsaturated ketones **7** are formed from dihydrofurans **3** through an acid-promoted transformation (Scheme 6) and not from the cationic intermediate **C**, as reported by many authors.[9a,49,54a,56,57,68a,c,d,69c]

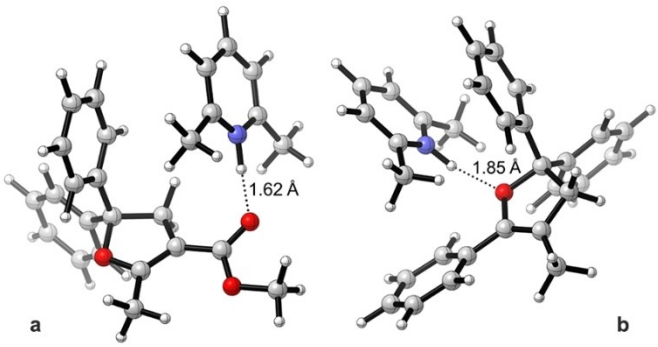

Figure 5. DFT optimized structures of the final products **3aa/LUTH$^+$** (**a**) and **3ga/LUTH$^+$** (**b**).

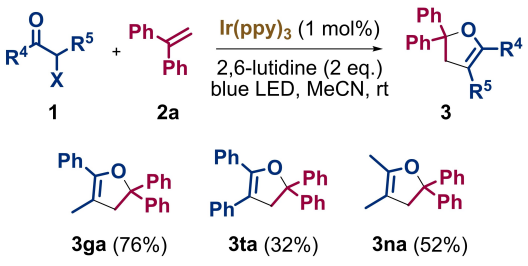

Scheme 8. Reaction conditions: **1** (1.2 eq.), **2a** (0.1 mmol), $Ir(ppy)_3$ (1 mol%), 2,6-lutidine (2 eq.), MeCN (1 mL), blue LED (465 nm), freeze pump thaw (1 cycle), rt, 24 h. NMR yields determined by ^{1}H NMR spectroscopic analysis of the crude mixture using triphenylmethane as internal standard and integrating the signals of the products.

Conclusion

In summary, we have developed the first example of visible light-promoted photoredox catalytic reaction between α-halo ketones **1** and alkenes **2** showing a predictable chemodivergent outcome. 2,3-Dihydrofurans **3** or β,γ-unsaturated ketones **7** were obtained mainly depending on the substrate substitution pattern. However, the role played by the reaction conditions was disclosed thanks to the identification of a plausible reaction mechanism, based on careful experimental investigations and DFT calculations. Concerning the proposed mechanistic hypothesis, two features of this transformation deserve to be emphasized: *i*) the process is configured as a radical-polar crossover reaction, in which radical species are initially generated and then converted into reactive cationic intermediates, *ii*) the transformation is redox-neutral, acting the Ir-catalyst as both reductant and oxidant in two different steps of the process. The mild reaction conditions and the redox-neutral nature of the transformation make it particularly sustainable avoiding the use of both sacrificial reactants and stoichiometric strong oxidants, sometimes expensive, potentially environmentally unfriendly and/or source of side-reactions.

The developed protocol represents the first example of photoredox catalytic coupling between α-haloketones and unfunctionalized olefins providing variably substituted β,γ-alkenyl ketones in good yields, avoiding their rearrangement into the α,β-unsaturated derivatives. Moreover, our approach offers a particularly straightforward synthesis of cyclic hemiketals (**6**), characterized by a tetrahydrofuran skeleton with three quaternary carbons, which were obtained for the first time in high yield by radical addition of ketones to olefins.

Experimental Section

General Information

All the commercial chemicals were purchased from Sigma-Aldrich, VWR, Alfa Aesar, or TCI-Chemicals and used without additional purifications. The ^{1}H and ^{13}C NMR spectra were recorded on a Varian INOVA 400 NMR instrument with a 5 mm probe. All chemical shifts have been quoted relative to residue solvent signal; chemical shifts (δ) are reported in ppm and coupling constants (J) are reported in hertz (Hz). HPLC analyses were performed on an Agilent Technologies HP1100 instrument. A Phenomenex Gemini C18 3 µm (100×3 mm) column was employed for the chromatographic separation: mobile phase H_2O/CH_3CN, gradient from 30% to 80% of CH_3CN in 8 min, 80% of CH_3CN until 22 min, then up to 90%

of CH_3CN in 2 min, flow rate 0.4 mL min^{-1}. Low-resolution MS (LRMS) ESI analyses were performed on an Agilent Technologies MSD1100 single-quadrupole mass spectrometer. Mass spectrometric detection was performed in the full-scan mode from *m/z* 50 to 2500, with a scan time of 0.1 s in the positive ion mode, ESI spray voltage of 4500 V, nitrogen gas pressure of 35 psi, drying gas flow rate of 11.5 mL min^{-1} and fragmentor voltage of 30 V. High-resolution MS (HRMS) ESI analyses were performed on a Xevo G2-XS QTof (Waters) mass spectrometer. Mass spectrometric detection was performed in the full-scan mode from *m/z* 50 to 1200, with a scan time of 0.15 s in the positive ion mode, cone voltage: 40 V, collision energy: 6.00 eV. ESI: capillary: 3 kV, cone: 40 V, source temperature: 120 °C, desolvation temperature: 600 °C, cone gas flow: 50 L/h, desolvation gas flow: 1000 L/h. Melting point (m.p.) measurements were performed on Bibby Stuart Scientific SMP3 apparatus. Flash chromatography purifications were carried out using VWR silica gel (40–63 µm particle size). Thin-layer chromatography was performed on Merck 60 F254 plates.

Typical Procedure for the Photoredox Synthesis of Products 3, 6 and 7

All reactions were performed on 0.1 mmol scale of olefin **2** (or halogenated compound **1** when an excess of alkene was used). A 4 mL screw cap septum vial equipped with a magnetic stirring bar was charged with the olefin **2** (0.1 mmol), MeCN (1 mL), the halogenated compound **1** (1.2 equivalents), Na_2HPO_4 (1 equivalent) and $Ir(ppy)_3$ (1 mol%). The vial was closed and the oxygen was removed by one cycle of the freeze-pump-thaw procedure, then the vial was filled with argon. The reaction mixture was irradiated under strong stirring using blue LED stripes (465 nm) for 24 h unless otherwise stated. Eventually, the inorganic solid was filtered through a cotton plug and the solvent was removed under reduced pressure. The crude mixture was analyzed by ^{1}H NMR spectroscopy using triphenylmethane (0.1 mmol) as an internal standard. The product was then purified by flash chromatography on silica gel.

For the reactions carried out in the presence of water, the work-up was as follows: EtOAc (1 mL) was added and the two phases were separated. The aqueous phase was extracted two more times with EtOAc (2×2 mL), the combined organic phases were collected, dried over Na_2SO_4 and filtered. The solvent was evaporated under reduced pressure.

Acknowledgements

We acknowledge Ministero dell'Università e della Ricerca (PRIN2017 – 20174SYJAF_001, SURSUMCAT) and University of Bologna (RFO) for the financial support.

References

[1] a) B. T. Sharipov, F. A. Valeev, *Chem. Heterocycl. Compd.* **2020**, *56*, 982–989; b) W. B. Mors, M. C. Nascimento, J. P. Parente, M. H. Silva, P. A. Melo, G. Suarez-Kurtz, *Toxicon* **1989**, *27*, 1003–1009; c) M. J. Somerville, P. L. Katavic, L. K. Lambert, G. K. Pierens, J. T. Blanchfield, G. Cimino, E. Mollo, M. Gavagnin, M. G. Banwell, Mary J. Garson, *J. Nat. Prod.* **2012**, *75*, 1618–1624; d) X. Cheng, C. D. Quintanilla, L. Zhang, *J. Org. Chem.* **2019**, *84*, 11054–11060; e) R. B. Von Dreele, G. R. Pettit, R. H. Ode, R. E. Perdue Jr., J. D. White, P. S. Manchand, *J. Am. Chem. Soc.* **1975**, *97*, 6236–6240; f) S. J. Sinmondsc, R. Botanic, *Tetrahedron Lett.* **1987**, *28*, 221–224.

[2] a) S. Sari, M. Yilmaz, *Med. Chem. Res.* **2020**, *29*, 1804–1818; b) K. Frydenvang, D. S. Pickering, G. U. Kshirsagar, G. U. Kshirsagar, G. Chemi, S. Gemma, D. Sprogøe, A. M. Kærn, S. Brogi, G. Campiani, S. Butini, J. S. Kastrup, *ACS Chem. Neurosci.* **2020**, *11*, 1791–1800; c) K. Sugimoto, K. Tamura, N. Ohta, C. Tohda, N. Toyooka, H. Nemoto, Y. Matsuya, *Bioorg. Med. Chem. Lett.* **2012**, *22*, 449–452; d) S. H. Kurma, S. Karri, M. Kuncha, R. Sistla, C. R. Bhimapaka, *Bioorg. Med. Chem. Lett.* **2020**, *30*, 127341; e) Y. Zhang, H. Zhong, T. Wang, D. Geng, M. Zhang, K. Li, *Eur. J. Med. Chem.* **2012**, *48*, 69–80; f) T. Koike, T. Takai, Y. Hoashi, M. Nakayama, Y. Kosugi, M. Nakashima, S. I. Yoshikubo, K. Hirai, O. Uchikawa, *J. Med. Chem.* **2011**, *54*, 4207–4218; g) J. Kashanna, R. A. Kumar, R. Kishore, D. N. Kumar, A. S. Kumar, *Chem. Biodiversity* **2018**, *15*, e1800277; h) J. M. Madar, L. A. Shastri, S. L. Shastri, M. Holiyachi, N. S. Naik, F. Shaikh, V. M. Kumbar, K. G. Bhat, S. D. Joshi, V. A. Sungar, *ChemistrySelect* **2018**, *3*, 10738–10749; i) H. A. Oketch-Rabah, E. Lemmich, S. F. Dossaji, T. G. Theander, C. E. Olsen, C. Cornett, A. Kharazmi, S. B. Christensen, *J. Nat. Prod.* **1997**, *60*, 458–461.

[3] a) Z. Chen, A. Zhang, H. Xiao, F. Huo, Z. Zhen, X. Liu, S. Bo, *Dyes Pigm.* **2020**, *173*, 107876; b) J. E. Baumeister, K. M. Reinig, C. L. Barnes, S. P. Kelley, S. S. Jurisson, *Inorg. Chem.* **2018**, *57*, 12920–12933.

[4] a) R. Jacques, R. Pal, N. A. Parker, C. E. Sear, P. W. Smith, A. Ribaucourt, D. M. Hodgson, *Org. Biomol. Chem.* **2016**, *14*, 5875–5893; b) C. He, J. Cai, Y. Zheng, C. Pei, L. Qiu, X. Xu, *ACS Omega* **2019**, *4*, 15754–15763; c) T. Wang, M. Tamura, Y. Nakagawa, K. Tomishige, *ChemSusChem* **2019**, *12*, 3615–3626; d) T. R. M. Rezende, J. O. S. Varejão, A. L. L. D. A. Sousa, S. M. B. Castañeda, S. A. Fernandes, *Org. Biomol. Chem.* **2019**, *17*, 2913–2922; e) Y. Bin Shen, S. S. Li, Y. M. Sun, L. Yu, Z. H. Hao, Q. Liu, J. Xiao, *J. Org. Chem.* **2019**, *84*, 2779–2785; f) C. Grosso, M. Liber, A. F. Brigas, T. M. V. D. Pinho, E. Melo, A. Lemos, *J. Chem. Educ.* **2019**, *96*, 148–152; g) J.-B. Chen, M. Xu, J.-Q. Zhang, B.-B. Sun, J.-M. Hu, J.-Q. Yu, X.-W. Wang, Y. Xia, Z. Wang, *ACS Catal.* **2020**, *10*, 3556–3563; h) J. Mansot, J. Lauberteaux, A. Lebrun, M. Mauduit, J.-J. Vasseur, R. M. de Figueiredo, S. Arseniyadis, J.-M. Campagne, M. Smietana, *Chem. Eur. J.* **2020**, *26*, 3519–3523; i) A. Romero-Arenas, V. Hornillos, J. Iglesias-Sigüenza, R. Fernández, J. López-Serrano, A. Ros, J. M. Lassaletta, *J. Am. Chem. Soc.* **2020**, *142*, 2628–2639.

[5] J. D. Feist, Y. Xia, *J. Am. Chem. Soc.* **2020**, *142*, 1186–1189.
[6] T. G. Kilroy, T. P. O'Sullivan, P. J. Guiry, *Eur. J. Org. Chem.* **2005**, 4929–4949.
[7] M. A. Calter, C. Zhu, *Org. Lett.* **2002**, *4*, 205–208.
[8] a) R. Çalişkan, T. Pekel, W. H. Watson, M. Balci, *Tetrahedron Lett.* **2005**, *46*, 6227–6230; b) F. Garzino, A. Méou, P. Brun, *Tetrahedron Lett.* **2000**, *41*, 9803–9807; c) R. Çalışkan, B. Alabaş, *Tetrahedron* **2019**, *75*, 1–7; d) B. Hocaoglu, M. Yilmaz, *Synth. Commun.* **2019**, *49*, 1938–1946; e) H. Nishino, *Bull. Chem. Soc. Jpn.* **1985**, *58*, 1922–1927.
[9] a) Y. Zhang, A. J. Raines, R. A. Flowers, *Org. Lett.* **2003**, *5*, 2363–2365; b) Y. R. Lee, B. S. Kim, D. H. Kim, *Tetrahedron* **2000**, *56*, 8845–8853; c) M. G. Vinogradov, A. E. Kondorsky, G. I. Nikishin, *Synthesis* **1988**, 60–62.
[10] Y. Wang, S. Zhu, *Tetrahedron* **2001**, *57*, 3383–3387.
[11] L. Xia, Y. R. Lee, *Adv. Synth. Catal.* **2013**, *355*, 2361–2374.
[12] T. Shi, S. Teng, Y. Wei, X. Guo, W. Hu, *Green Chem.* **2019**, *21*, 4936–4940.
[13] a) T. Naveen, R. Kancherla, D. Maiti, *Org. Lett.* **2014**, *16*, 5446–5449; b) S. Yang, Y. Li, Q. Zhang, *Chin. J. Org. Chem.* **2019**, *39*, 2226–2234; c) H. Yi, Z. Liao, G. Zhang, G. Zhang, C. Fan, X. Zhang, E. E. Bunel, C. W. Pao, J. F. Lee, A. Lei, *Chem. Eur. J.* **2015**, *21*, 18925–18929.
[14] H. Liu, Z. Sun, K. Xu, Y. Zheng, D. Liu, W. Zhang, *Org. Lett.* **2020**, *22*, 4680–4685.
[15] S. Wang, L. Y. He, L. N. Guo, *Synthesis* **2015**, *47*, 3191–3197.
[16] T. Y. Ko, S. W. Youn, *Adv. Synth. Catal.* **2016**, *358*, 1934–1941.
[17] S. Tang, K. Liu, Y. Long, X. Gao, M. Gao, A. Lei, *Org. Lett.* **2015**, *17*, 2404.
[18] M. Xiong, X. Liang, X. Liang, Y. Pan, A. Lei, *ChemElectroChem* **2019**, *6*, 3383–3386.
[19] a) V. Mane, S. T. Sivanandan, R. G. Santana, A. Beatriz, E. N. Da Silva Júnior, I. N. N. Namboothiri, *J. Org. Chem.* **2020**, *85*, 8825–8843; b) D. Becerra, W. Raimondi, D. Dauzonne, T. Constantieux, D. Bonne, J. Rodriguez, *Synthesis* **2017**, *49*, 195–201; c) M. Balha, B. Mondal, S. C. Pan, *Org. Biomol. Chem.* **2019**, *17*, 6557–6561.
[20] Z. Sun, Z. Li, W. W. Liao, *Green Chem.* **2019**, *21*, 1614–1618.
[21] L. J. Chen, J. H. Yu, B. He, J. W. Xie, Y. X. Liu, W. D. Zhu, *J. Org. Chem.* **2020**, *85*, 7793–7802.
[22] P. K. Warghude, A. S. Sabale, R. G. Bhat, *Org. Biomol. Chem.* **2020**, *18*, 1794–1799.
[23] a) F. L. Zhu, Y. H. Wang, D. Y. Zhang, J. Xu, X. P. Hu, *Angew. Chem. Int. Ed.* **2014**, *53*, 10223–10227; *Angew. Chem.* **2014**, *126*, 10387–10391; b) P. A. Sakharov, N. V. Rostovskii, A. F. Khlebnikov, T. L. Panikorovskii, M. S. Novikov, *Org. Lett.* **2019**, *21*, 3615–3619; c) X. Li, C. Han, Y. Huang, H. Yao, A. Lin, *Org. Chem. Front.* **2019**, *6*, 245–248.
[24] a) T. Li, L. Zhang, *J. Am. Chem. Soc.* **2018**, *140*, 17439–17443; b) T. Li, Y. Yang, B. Li, X. Bao, L. Zhang, *Org. Lett.* **2019**, *21*, 7791–7794; c) S. Fernández, J. Santamaría, A. Ballesteros, *Org. Lett.* **2020**, *22*, 6590–6594.
[25] a) J. Liu, Q. Y. Liu, X. X. Fang, G. Q. Liu, Y. Ling, *Org. Biomol. Chem.* **2018**, *16*, 7454–7460; b) L. N. Guo, S. Wang, X. H. Duan, S. L. Zhou, *Chem. Commun.* **2015**, *51*, 4803–4806; c) X. Bai, L. Lv, Z. Li, *Org. Chem. Front.* **2016**, *3*, 804–808; d) Z. Guan, Y. Wang, H. Wang, Y. Huang, S. Wang, H. Tang, H. Zhang, A. Lei, *Green Chem.* **2019**, *21*, 4976–4980.
[26] a) J. L. Zhou, L. J. Wang, H. Xu, X. L. Sun, Y. Tang, *ACS Catal.* **2013**, *3*, 685–688; b) Z. Chen, J. Zhang, *Chem. Asian J.* **2010**, *5*, 1542–1545; c) F. Seyma Gungor, G. Merey, O. Anac, *ChemistrySelect* **2020**, *5*, 5337–5340; d) J. W. Kang, X. Li, F. Y. Chen, Y. Luo, S. C. Zhang, B. Kang, C. Peng, X. Tian, B. Han, *RSC Adv.* **2019**, *9*, 12255–12264.
[27] a) X. Liang, P. Guo, W. Yang, M. Li, C. Jiang, W. Sun, T. P. Loh, Y. Jiang, *Chem. Commun.* **2020**, *56*, 2043–2046; b) S. Ma, L. Lu, J. Zhang, *J. Am. Chem. Soc.* **2004**, *126*, 9645–9660; c) M. Li, S. Lin, Z. Dong, X. Zhang, F. Liang, J. Zhang, *Org. Lett.* **2013**, *15*, 3978–3981; d) V. K. Yadav, R. Balamurugan, *Org. Lett.* **2001**, *3*, 2717–2718; e) Y. Wang, J. Han, J. Chen, W. Cao, *Chem. Commun.* **2016**, *52*, 6817–6820.
[28] D. Zhang, Z. Kang, J. Liu, W. Hu, *Science* **2019**, *14*, 292–300.
[29] J. Xin, W. Zhu, B. Ye, T. Lu, T. Hayashi, X. Dou, *ACS Catal.* **2020**, *10*, 2958–2963.
[30] a) L. Cerisoli, M. Lombardo, C. Trombini, A. Quintavalla, *Chem. Eur. J.* **2016**, *22*, 3865–3872; b) A. Quintavalla, *Curr. Med. Chem.* **2018**, *25*, 917–962; c) M. Ortalli, S. Varani, C. Rosso, A. Quintavalla, M. Lombardo, C. Trombini, *Eur. J. Med. Chem.* **2019**, *170*, 126–140; d) M. Persico, R. Fattorusso, O. Taglialatela-Scafati, G. Chianese, I. De Paola, L. Zaccaro, F. Rondinelli, M. Lombardo, A. Quintavalla, C. Trombini, E. Fattorusso, C. Fattorusso, B. Farina, *Sci. Rep.* **2017**, *7*, 1–11; e) M. Ortalli, S. Varani, G. Cimato, R. Veronesi, A. Quintavalla, M. Lombardo, M. Monari, C. Trombini, *J. Med. Chem.* **2020**, *63*, 13140–13158.
[31] a) T. Rigotti, J. Alemán, *Chem. Commun.* **2020**, *56*, 11169–11190; b) C. Prentice, J. Morrisson, A. D. Smith, E. Zysman-Colman, *Beilstein J. Org. Chem.* **2020**, *16*, 2363–2441; c) T. H. Rehm, *Chem. Eur. J.* **2020**, *26*, 16952–16974; d) L. Fensterbank, J. P. Goddard, C. Ollivier, *Visible Light Photocatal. Org. Chem.* **2017**, 25–71; e) F. Strieth-Kalthoff, M. J. James, M. Teders, L. Pitzer, F. Glorius, *Chem. Soc. Rev.* **2018**, *47*, 7190–7202; f) L. Marzo, S. K. Pagire, O. Reiser, B. König, *Angew. Chem. Int. Ed.* **2018**, *57*, 10034–10072; *Angew. Chem.* **2018**, *130*, 10188–10228; g) Y. Q. Zou, F. M. Hörmann, T. Bach, *Chem. Soc. Rev.* **2018**, *47*, 278–290; h) D. Staveness, I. Bosque, C. R. J. Stephenson, *Acc. Chem. Res.* **2016**, *49*, 2295–2306; i) *Visible Light Photocatalysis in Organic Chemistry*, (Eds.: C. Stephenson, T. Yoon, D. W. C. MacMilllan), Wiley-VCH, Weinheim, **2018**;

j) I. K. Sideri, E. Voutyritsa, C. G. Kokotos, *Org. Biomol. Chem.* **2018**, *16*, 4596–4614.
[32] W. Xia, C. Yang, B. O. Patrick, J. R. Scheffer, C. Scott, *J. Am. Chem. Soc.* **2005**, *127*, 2725–2730.
[33] a) X. J. Wei, D. T. Yang, L. Wang, T. Song, L. Z. Wu, Q. Liu, *Org. Lett.* **2013**, *15*, 6054–6057; b) I. Triandafillidi, M. G. Kokotou, C. G. Kokotos, *Org. Lett.* **2018**, *20*, 36–39.
[34] E. Speckmeier, P. J. W. Fuchs, K. Zeitler, *Chem. Sci.* **2018**, *9*, 7096–7103.
[35] a) H. Jiang, Y. Cheng, Y. Zhang, S. Yu, *Org. Lett.* **2013**, *15*, 4884–4887; b) S. Wang, W. L. Jia, L. Wang, Q. Liu, L. Z. Wu, *Chem. Eur. J.* **2016**, *22*, 13794–13798; c) J. Cheng, Y. Cheng, J. Xie, C. Zhu, *Org. Lett.* **2017**, *19*, 6452–6455.
[36] a) R. R. Liu, J. J. Hong, C. J. Lu, M. Xu, J. R. Gao, Y. X. Jia, *Org. Lett.* **2015**, *17*, 3050–3053; b) M. Ghosh, S. Mishra, K. Monir, A. Hajra, *Org. Biomol. Chem.* **2015**, *13*, 309–314; c) M. Ghosh, S. Mishra, A. Hajra, *J. Org. Chem.* **2015**, *80*, 5364–5368; d) K. Koga, *Bull. Chem. Soc. Jpn.* **1998**, 475–482; e) Y. Jiang, V. Z. Y. Khong, E. Lourdusamy, C. M. Park, *Chem. Commun.* **2012**, *48*, 3133–3135.
[37] G. Fumagalli, S. Boyd, M. F. Greaney, *Tetrahedron Lett.* **2015**, *56*, 2571–2573.
[38] a) W. E. Fristad, J. R. Peterson, *J. Org. Chem.* **1985**, *50*, 10; b) D. Liu, S. Tang, H. Yi, C. Liu, X. Qi, Y. Lan, A. Lei, *Chem. Eur. J.* **2014**, *20*, 15605–15610.
[39] E. Areo, E. Montroni, P. Melchiorre, *Angew. Chem. Int. Ed.* **2014**, *53*, 12064–12068.
[40] E. C. Gentry, R. R. Knowles, *Acc. Chem. Res.* **2016**, *49*, 1546–1556.
[41] R. V. Hoffman, W. S. Weiner, N. Maslouh, *J. Org. Chem.* **2001**, *66*, 5790–5795.
[42] C. K. Prier, D. A. Rankic, D. W. C. MacMillan, *Chem. Rev.* **2013**, *113*, 5322–5363.
[43] N. A. Romero, D. A. Nicewicz, *Chem. Rev.* **2016**, *116*, 10075–10166.
[44] E. Speckmeier, T. G. Fischer, K. Zeitler, *J. Am. Chem. Soc.* **2018**, *140*, 15353–15365.
[45] a) Gualandi, A. Nenov, M. Marchini, G. Rodeghiero, I. Conti, E. Paltanin, M. Balletti, P. Ceroni, M. Garavelli, P. G. Cozzi, *ChemCatChem* **2021**, *13*, 981–989.
[46] E. Baciocchi, R. Ruzziconi, *J. Org. Chem.* **1991**, *56*, 4772–4778.
[47] Y. Zhou, F. L. Zhu, Z. T. Liu, X. M. Zhou, X. P. Hu, *Org. Lett.* **2016**, *18*, 2734–2737.
[48] J. Aponte-Guzmán, L. H. Phun, M. A. Cavitt, J. E. Taylor, J. C. Davy, S. France, *Chem. Eur. J.* **2016**, *22*, 10405–10409.
[49] H. Jiang, C. Huang, J. Guo, C. Zeng, Y. Zhang, S. Yu, *Chem. Eur. J.* **2012**, *18*, 15158–15166.
[50] a) M. Yilmaz, A. Tarik Pekel, *Synth. Commun.* **2001**, *31*, 2189–2194; b) B. M. Casey, C. A. Eakin, J. Jiao, D. V. Sadasivam, R. A. Flowers, *Tetrahedron* **2009**, *65*, 10762–10768; c) X. H. Ouyang, C. Hu, R. J. Song, J. H. Li, *Org. Lett.* **2018**, *20*, 4659–4662; d) E. I. Heiba, R. M. Dessau, *J. Am. Chem. Soc.* **1972**, *94*, 2888–2889; e) B. B. Snider, *Chem. Rev.* **1996**, *96*, 339–363.
[51] P. Li, J. Zhao, C. Xia, F. Li, *Org. Lett.* **2014**, *16*, 5992–5995.
[52] a) S. Choi, J. Park, E. Yu, J. Sim, C. M. Park, *Angew. Chem. Int. Ed.* **2020**, *59*, 11886–11891; *Angew. Chem.* **2020**, *132*, 11984–11989; b) S. Choi, H. Oh, J. Sim, E. Yu, S. Shin, C. M. Park, *Org. Lett.* **2020**, *22*, 5528–5534; c) G. Lu, B. Lin, Y. Gao, J. Ying, G. Tang, Y. Zhao, *Synlett* **2017**, *28*, 724–728.
[53] H. Y. Lee, K. Lee, J. H. Hah, D. K. Moon, C. K. Lee, *Bull. Korean Chem. Soc.* **2010**, *31*, 2139–2140.
[54] a) Q. Liu, H. Yi, J. Liu, Y. Yang, X. Zhang, Z. Zeng, A. Lei, *Chem. Eur. J.* **2013**, *19*, 5120–5126; b) *Advances in Free Radical Chemistry*, (Ed.: S. Z. Zard) JAI Press, Greenwich, CT, **2000**.
[55] E. P. Farney, S. J. Chapman, W. B. Swords, M. D. Torelli, R. J. Hamers, T. P. Yoon, *J. Am. Chem. Soc.* **2019**, *141*, 6385–6391.
[56] Y. Zhang, A. J. Raines, R. A. Flowers, *J. Org. Chem.* **2004**, *69*, 6267–6272.
[57] J. R. Hwu, C. N. Chen, S. S. Shiao, *J. Org. Chem.* **1995**, *60*, 856–862.
[58] T. Nishikata, K. Itonaga, N. Yamaguchi, M. Sumimoto, *Org. Lett.* **2017**, *19*, 2686–2689.
[59] Y. Deng, G. Zhang, X. Qi, C. Liu, J. T. Miller, A. J. Kropf, E. E. Bunel, Y. Lan, A. Lei, *Chem. Commun.* **2015**, *51*, 318–321.
[60] J. D. Nguyen, J. W. Tucker, M. D. Konieczynska, C. R. J. Stephenson, *J. Am. Chem. Soc.* **2011**, *133*, 4160–4163.
[61] a) S. Minegishi, R. Loos, S. Kobayashi, H. Mayr, *J. Am. Chem. Soc.* **2005**, *127*, 2641–264; b) S. Minegishi, S. Kobayashi, H. Mayr, *J. Am. Chem. Soc.* **2004**, *126*, 5174–5181.
[62] C. J. Wallentin, J. D. Nguyen, P. Finkbeiner, C. R. J. Stephenson, *J. Am. Chem. Soc.* **2012**, *134*, 8875–8884.
[63] a) E. J. Woo, C. M. Starks, J. R. Carney, R. Arslanian, L. Cadapan, S. Zavala, P. Licari, *J. Antibiot.* **2002**, *55*, 141–146; b) K. Sugawara, Y. Nlshiyama, S. Toda, N. Komiyama, M. Hatori, T. Moriyama, Y. Sawada, H. Kamei, M. Konishi, T. Oki, *J. Antibiot.* **1992**, *45*, 1433–1441; c) K. T. Andrews, A. Walduck, M. J. Kelso, D. P. Fairlie, A. Saul, P. G. Parsons, *Int. J. Parasitol.* **2000**, *30*, 761–768; d) N. Mishra, D. R. Brown, I. M. Olorenshaw, G. M. Kammer, *Proc. Natl. Acad. Sci. USA* **2001**, *98*, 2628–2633; e) M. S. Finnin, J. R. Donigian, A. Cohen, V. M. Richon, R. A. Rifkind, P. A. Marks, R. Breslow, N. P. Pavletich, *Nature* **1999**, *401*, 188–193; f) M. B. Ksebati, F. J. Schmitz, *J. Org. Chem.* **1985**, *50*, 5637–5642; g) T. Wakabayashi, K. Mori, S. Kobayashi, *J. Am. Chem. Soc.* **2001**, *123*, 1372–1375; h) S. M. Mandala, R. A. Thornton, M. Rosenbach, J. Milligan, M. Garcia-Calvo, H. G. Bull, M. B. Kurtz, *J. Biol. Chem.* **1997**, *272*, 32709–32714.
[64] a) X. Yang, F. D. Toste, *J. Am. Chem. Soc.* **2015**, *137*, 3205–3208; b) I. Iriarte, O. Olaizola, S. Vera, I. Gamboa, M. Oiarbide, C. Palomo, *Angew. Chem. Int. Ed.* **2017**, *56*, 8860–8864; *Angew. Chem.* **2017**, *129*, 8986–8990;

c) P. S. Akula, B. C. Hong, G. H. Lee, *Org. Lett.* **2018**, *20*, 7835–7839; d) X. Kong, J. Song, J. Liu, M. Meng, S. Yang, M. Zeng, X. Zhan, C. Li, X. Fang, *Chem. Commun.* **2018**, *54*, 4266–4269; e) X. Li, X. Kong, S. Yang, M. Meng, X. Zhan, M. Zeng, X. Fang, *Org. Lett.* **2019**, *21*, 1979–1983; f) I. Urruzuno, O. Mugica, G. Zanella, S. Vera, E. Gómez-Bengoa, M. Oiarbide, C. Palomo, *Chem. Eur. J.* **2019**, *25*, 9701–9709; g) D. A. Shabalin, E. V. Ivanova, I. A. Ushakov, E. Y. Schmidt, B. A. Trofimov, *J. Org. Chem.* **2020**, *85*, 8429–8436.

[65] a) S. Undeela, J. P. Ramchandra, R. S. Menon, *Tetrahedron Lett.* **2014**, *55*, 5667–5670; b) E. Y. Schmidt, I. V. Tatarinova, E. V. Ivanova, B. A. Trofimov, *Mendeleev Commun.* **2017**, *27*, 283–284.

[66] a) M. Grigalunas, T. Ankner, P. O. Norrby, O. Wiest, P. Helquist, *Org. Lett.* **2014**, *16*, 3970–3973; b) M. Grigalunas, T. Ankner, P. O. Norrby, O. Wiest, P. Helquist, *J. Am. Chem. Soc.* **2015**, *137*, 7019–7022; c) Y. Zaid, C. D. Mboyi, M. P. Drapeau, L. Radal, F. O. Chahdi, Y. K. Rodi, T. Ollevier, M. Taillefer, *Org. Lett.* **2019**, *21*, 1564–1568; d) A. M. Taylor, R. A. Altman, S. L. Buchwald, *J. Am. Chem. Soc.* **2009**, *131*, 9900–9901; e) J. Huang, E. Bunel, M. M. Faul, *Org. Lett.* **2007**, *9*, 4343–4346; f) T. Ankner, C. C. Cosner, P. Helquist, *Chem. Eur. J.* **2013**, *19*, 1858–1871.

[67] a) T. Xu, X. Hu, *Angew. Chem. Int. Ed.* **2015**, *54*, 1307–1311; *Angew. Chem.* **2015**, *127*, 1323–1327; b) D. Wang, J. Wu, J. Huang, J. Liang, P. Peng, H. Chen, F. Wu, *Tetrahedron* **2017**, *73*, 3478–3484; c) X. Wang, J. Hu, J. Ren, T. Wu, J. Wu, F. Wu, *Tetrahedron* **2019**, *75*, 2–9; d) J. Liang, G. Huang, P. Peng, T. Zhang, J. Wu, F. Wu, *Adv. Synth. Catal.* **2018**, *360*, 2221–2227; e) C. Che, H. Zheng, G. Zhu, *Org. Lett.* **2015**, *17*, 1617–1620.

[68] a) C. Liu, S. Tang, D. Liu, J. Yuan, L. Zheng, L. Meng, A. Lei, *Angew. Chem. Int. Ed.* **2012**, *51*, 3638–3641; *Angew. Chem.* **2012**, *124*, 3698–3701; b) G. K. Friestad, Y. Wu, *Org. Lett.* **2009**, *11*, 819–822; c) C. Yu, N. Iqbal, S. Park, E. J. Cho, *Chem. Commun.* **2014**, *50*, 12884–12887; d) T. Nishikata, G. Hirata, T. Shimada, *Org. Lett.* **2020**, *22*, 8952–8956.

[69] a) Y. Yamane, K. Yoshinaga, M. Sumimoto, T. Nishikata, *ACS Catal.* **2019**, *9*, 1757–1762; b) R. Ding, Z. D. Huang, Z. L. Liu, T. X. Wang, Y. H. Xu, T. P. Loh, *Chem. Commun.* **2016**, *52*, 5617–5620, 5617; c) T. Nishikata, Y. Noda, R. Fujimoto, T. Sakashita, *J. Am. Chem. Soc.* **2013**, *135*, 16372–16375; d) C. Tang, R. Zhang, B. Zhu, J. Fu, Y. Deng, L. Tian, W. Guan, X. Bi, *J. Am. Chem. Soc.* **2018**, *140*, 16929–16935; e) C. Qu, Z. Wu, W. Li, H. Du, C. Zhu, *Adv. Synth. Catal.* **2017**, *359*, 1672–1677; f) X. Wang, S. Zhao, J. Liu, D. Zhu, M. Guo, X. Tang, G. Wang, *Org. Lett.* **2017**, *19*, 4187–4190.

[70] B. A. Sim, D. Griller, D. D. M. Wayner, *J. Am. Chem. Soc.* **1989**, *111*, 754–755.

[71] a) S. M. Gibson, J. M. D'Oyley, J. I. Higham, K. Sanders, V. Laserna, A. E. Aliev, T. D. Sheppard, *Eur. J. Org. Chem.* **2018**, 4018–4028; b) H. Ito, A. Sato, T. Kobayashi, T. Taguchi, *Chem. Commun.* **1998**, 2441–2442.

[72] T. Kumon, S. Hashishita, T. Kida, S. Yamada, T. Ishihara, T. Konno, *Beilstein J. Org. Chem.* **2017**, *14*, 148–154.

[73] a) K. T. O'Brien, J. W. Nadraws, A. B. Smith III, *Org. Lett.* doi.org/10.1021/acs.orglett.0c03508; b) L. Bonnac, S. E. Lee, G. T. Giuffredi, L. M. Elphick, A. A. Anderson, E. S. Child, D. J. Mann, V. Gouverneur, *Org. Biomol. Chem.* **2010**, *8*, 1445–1454; c) B. Linclau, A. J. Boydell, R. S. Timofte, K. J. Brown, V. Vinader, A. C. Weymouth-Wilson, *Org. Biomol. Chem.* **2009**, *7*, 803–814; d) J. Mulzer, D. Riether, *Tetrahedron Lett.* **1999**, *40*, 6197–6199; e) L. A. Paquette, P. E. Wiedeman, P. C. Bulman-Page, *J. Org. Chem.* **1988**, *53*, 1441–1450.

[74] B. B. Snider, L. Han, *Synth. Commun.* **1995**, *25*, 2337–2347.

[75] S. Yamada, S. Hashishita, T. Asai, T. Ishihara, T. Konno, *Org. Biomol. Chem.* **2017**, *15*, 1495–1509.

[76] C. Sandford, M. A. Edwards, K. J. Klunder, D. P. Hickey, M. Li, K. Barman, M. S. Sigman, H. S. White, S. D. Minteer, *Chem. Sci.* **2019**, *10*, 6404–6422.

[77] a) D. M. Arias-Rotondo, J. K. McCusker, *Chem. Soc. Rev.* **2016**, *45*, 5803–5820; b) B. Brunschwig, N. Sutin, *J. Am. Chem. Soc.* **1978**, *100*, 7568–7577; c) J. N. Demas, E. W. Harris, R. P. McBride, *J. Am. Chem. Soc.* **1977**, *99*, 3547–3551.

[78] a) C. P. Andrieux, A. Le Gorande, J. M. Saveant, *J. Am. Chem. Soc.* **1992**, *114*, 17, 6892–6904; b) A. A. Isse, C. Y. Lin, M. L. Coote, A. Gennaro, *J. Phys. Chem. B* **2011**, *115*, 678–684; c) H. G. Roth, N. A. Romero, D. A. Nicewicz, *Synlett* **2016**, *27*, 714–723.

[79] a) D. D. M. Wayner, A. Houmam, *Acta Chem. Scand.* **1998**, *52*, 377–384; b) D. D. M. Wayner, D. J. McPhee, D. Griller, *J. Am. Chem. Soc.* **1988**, *110*, 132–137.

[80] M. M. Efremova, A. P. Molchanov, A. G. Larina, G. L. Starova, R. R. Kostikov, A. V. Stepakov, *Helv. Chim. Acta* **2016**, *99*, 487–493.

[81] T. Lund, D. D. M. Wayner, M. Jonsson, A. G. Larsen, K. Daasbjerg, *J. Am. Chem. Soc.* **2001**, *123*, 12590–12595.

[82] a) B. B. Snider, M. A. Dombroski, *J. Org. Chem.* **1987**, *52*, 5487–5489; b) L. Lv, S. Lu, Q. Guo, B. Shen, Z. Li, *J. Org. Chem.* **2015**, *80*, 698–704.